Lanthanum Hexaboride Nanoobelisks

Joseph Reese Brewer,[†] Nirmalendu Deo,[†] Y. Morris Wang,[§] and Chin Li Cheung*[,‡]

Department of Chemistry, University of Nebraska−Lincoln, Lincoln, Nebraska 68588, Nebraska Center for Materials and Nanoscience, Lincoln, Nebraska 68588, and Lawrence Livermore National Laboratory, Livermore, California 94550

Received August 15, 2007
Revised Manuscript Received October 16, 2007

Lanthanum hexaboride (LaB_6) is considered to be one of the most promising thermionic electron field emitting materials for use in electron microscopy and electron emitter productions because of its low work function (~2.6 eV), low volatility, and high brightness.[1,2] Geometric factors of the electron emitters such as shapes and aspect ratios have been found to greatly influence the local electric field at the tips and field emission current in various nanomaterials systems[3,4] such as silicon nanotips[5] and nanocones,[6] carbon nanotubes,[7] and zinc oxide nanowires.[8,9] However, systematic comparisons and detailed understanding of these geometric factors on the overall field enhancement factor are insufficient because of the difficulty in producing nanomaterials with different reproducible geometric tip shapes and diameters. Therefore, a methodology to produce materials of different shapes is expected to be beneficial for the advancement of nanomaterials as efficient field emitters.

The modified Fowler−Nordheim equation[10] predicts that electron emitters made of materials with high aspect ratio tips and low work function have greatly enhanced field emission current with low applied turn-on voltage. Wei et al. demonstrated this concept by experimentally proving that a lower turn-on voltage and higher emission current can be obtained from an individual multiwalled carbon nanotube tip coated with LaB_6 film than an unmodified one.[11] Recently, Zhang et al. synthesized LaB_6 nanowires with diameters varying from 20 nm to several hundred nanometers and examined their emission properties.[12,13] The reported emission current density of a nanowire with a 140 nm diameter at room temperature was found to be $\sim 5 \times 10^5$ A cm^{-2}, which is 1 order of magnitude higher than that of the state-of-the-art W/ZrO thermal field emitter at working conditions of 1800 °C and 3000 V. These nanowires also have an emission current density of the same order of magnitude as that of an individual CNT which is 10–50 times smaller in diameter. Although much thinner LaB_6 wires are predicted to have better field emission performance, these long, thin, and flexible structures may be undesirable for electron emitter sources in high-resolution electron microscopy. Structurally more robust materials with smaller tip diameters, such as cones, are less susceptible to thermal vibrations and mechanical stresses and are thus expected to provide better stability.[14] Furthermore, as in the case for carbon nanotubes, better control of tip shapes and diameters, which are crucial to the reproducibility of their emission property, have yet to be demonstrated for LaB_6 nanomaterials.[15]

Herein we report the synthesis of single-crystalline LaB_6 nanoobelisks with different pyramidal tip heights and diameters via a metal-catalyzed chemical vapor deposition method. A time trial growth study of these nanostructures suggests a possible multistage growth model to explain the shape of the as-synthesized materials. To the best of our knowledge, this is the first synthesis of LaB_6 nanostructures of nanoobelisk shapes with high-density array growth.

An adapted chemical vapor deposition (CVD) scheme via a vapor–liquid–solid (VLS) mechanism was applied to produce these nanostructures with preferred growth direction and much denser material growth than previously reported results.[12,13,16] The synthesis was based on the following chemical reaction

$$10LaCl_3(s) + 6B_{10}H_{14}(g) \rightarrow 10LaB_6(s) + 30HCl(g) + 27H_2(g)$$

Decaborane was used to synthesize the materials because it leads to a more thermodynamically favored reaction than boron halides used in previous syntheses of LaB_6 nanomaterials.[17] Because decaborane is solid at room temperature and can be sublimed at 70 °C, it is more convenient to handle than other gaseous or liquid boron precursors, which have much higher toxicity.

The synthesis was performed in a tube furnace at 1000 °C and a pressure of 160 mtorr for 13 min. The sublimed decaborane was introduced into a 1 in. quartz tube at a flow rate of 0.75 sccm and mixed with argon at a flow rate of 10 sccm. Precursor $LaCl_3$ (0.2 g, Sigma-Aldrich, Milwaukee,

* Corresponding author. E-mail: ccheung2@unl.edu.
[†] University of Nebraska−Lincoln.
[§] Lawrence Livermore National Laboratory.
[‡] Nebraska Center for Materials and Nanoscience.

(1) Swanson, L. W.; Gesley, M. A.; Davis, P. R. *Surf. Sci.* **1981**, *107*, 263.
(2) Gesley, M. A.; Swanson, L. W. *Surf. Sci.* **1984**, *146*, 583.
(3) Terrones, H.; Terrones, M. *New J. Phys.* **2003**, *5*, 126.
(4) Xu, N. S.; Huq, S. E. *Mater. Sci. Eng., R* **2005**, *48*, 47.
(5) Bai, X. D.; Zhia, C. Y.; Liu, S.; Wang, E. G.; Wang, Z. L. *Solid State Commun.* **2003**, *125*, 185.
(6) Cao, L.; Laim, L.; Ni, C.; Nabet, B.; Spanier, J. E. *J. Am. Chem. Soc.* **2005**, *127*, 13782.
(7) Wang, M. S.; Peng, L.-M.; Wang, J. Y.; Jin, C. H.; Chen, Q. *J. Phys. Chem. B* **2006**, *110*, 9397.
(8) Zhao, Q.; Zhang, H. Z.; Zhu, Y. W.; Feng, S. Q.; Sun, X. C.; Xu, J.; Yu, D. P. *Appl. Phys. Lett.* **2005**, *86*, 203115.
(9) Xu, C. X.; Sun, X. W.; Chen, B. J. *Appl. Phys. Lett.* **2004**, *84*, 1540.
(10) Vila, L.; Vincent, P.; Dauginet-De Pra, L.; Pirio, G.; Minoux, E.; Gangloff, L.; Demoustier-Champagne, S.; Sarazin, N.; Ferain, E.; Legras, R.; Piraux, L.; Legagneux, P. *Nano Lett.* **2004**, *4*, 521.
(11) Wei, W.; Jiang, K.; Wei, Y.; Liu, P.; Liu, K.; Zhang, L.; Li, Q.; Fan, S. *Appl. Phys. Lett.* **2006**, *89*, 203112.
(12) Zhang, H.; Tang, J.; Zhang, Q.; Zhao, G.; Yang, G.; Zhang, J.; Zhou, O.; Qin, L.-C. *Adv. Mater.* **2006**, *18*, 87.
(13) Zhang, H.; Zhang, Q.; Tang, J.; Qin, L.-C. *J. Am. Chem. Soc.* **2005**, *127*, 2862.
(14) Wei, C.; Srivastava, D. *Appl. Phys. Lett.* **2004**, *85*, 2208.
(15) Xu, J.; Zhao, Y.; Zou, C. *Chem. Phys. Lett.* **2006**, *423*, 138.
(16) Givargizov, E. I.; Obolenskaya, L. N. *J. Less-Common Met.* **1986**, *117*, 97.
(17) Peshev, P. *J. Solid State Chem.* **2000**, *154*, 157.

10.1021/cm702315x CCC: $37.00
Published on Web 11/16/2007

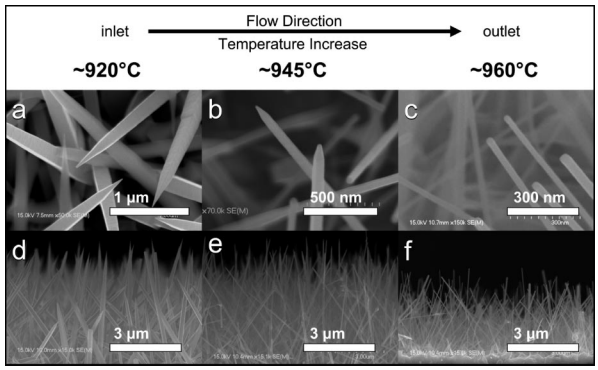

Figure 1. Typical SEM images of LaB_6 nanoobelisks and nanowires synthesized with substrates placed (a) 3, (b) 4, and (c) 5 cm downstream from the $LaCl_3$ precursors. (d−f) Zoom-out SEM images of the nanostructures in a−c, respectively.

WI) was placed on a quartz boat in the upstream end of the furnace. Silicon substrates (0.7 × 0.7 cm^2) coated with platinum (Pt) nanoparticles[18] of diameters 15–20 nm were placed on the same quartz boat at locations 3, 4, and 5 cm from the $LaCl_3$ in the downstream direction. The measured local temperatures of these three positions are about 920, 945, and 960 °C, respectively. The dark purple products were characterized with a JEOL JEM-2010 TEM with an Oxford EDX, a Phillips CM300 TEM with a GATAN image filter, and a Hitachi S4700 field-emission SEM. Elemental analysis at different regions of the nanoobelisks (tips, bulk shafts, and side edges) by energy-dispersive X-ray (EDX) was obtained in scanning transmission electron microscopy (STEM) mode.

The LaB_6 obelisk-shaped nanostructures are typically characterized by their rectangular pyramidal tops on four-sided shafts with wider bases. Nanoobelisks of different defined pyramidal top heights, cone angles, and shaft widths can be preferentially obtained by judicious placement of the substrates in a 2 cm long 920–945 °C growth zone downstream from the lanthanum precursor (Figure 1 and-Figure 2). At the lower-temperature growth zone (~920 °C) 3 cm downstream from the $LaCl_3$, preferential growth of nanoobelisks was obtained at a frequency of greater than 95%, with rectangular cross-sectioned nanorods accounting for the remaining structures (images a and d in Figure 1). The pyramidal top of these obelisks typically have tip diameters of 11 ± 5 nm, very sharp cone angles of 8.7° ± 1.3°, and heights of 753 ± 138 nm (Figure 2 and the Supporting Information, Figure S1). These obelisk shafts adopt a more tapered structure with length of ~4 μm, width of 150–250 nm at the base of the shaft, and angle of vertical declination of 0.8 ± 0.3°, characterized by a ~15% decrease in width over a 2 μm length (Figure 2d). High-density growth of these nanoobelisks can be routinely obtained (see the Supporting Information, Figure S2).

At a higher-temperature growth zone (~945 °C) 4 cm away from the La precursor, LaB_6 nanoobelisks with much shorter pyramidal tops and uniform width along the length of the shaft were obtained instead (images b and e in Figure

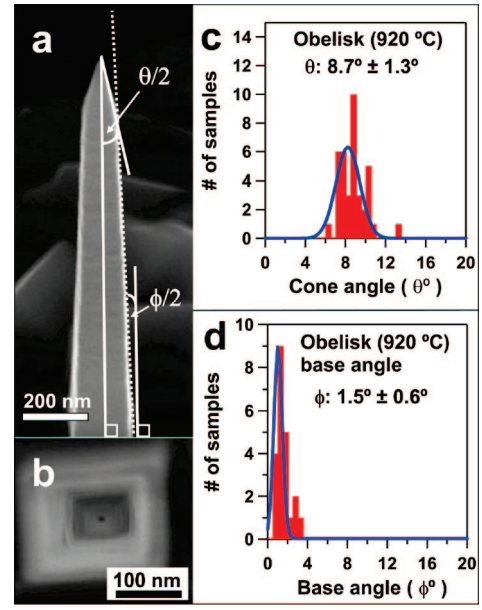

Figure 2. Typical SEM images of LaB_6 nanoobelisks grown at 920 °C and the statistics of corresponding cone angle measurements. SEM images of the (a) side view and (b) top view of a nanoobelisk. Histograms of (c) the cone angles at the pyramidal tips, θ, and (d) angle of vertical declination at the base, $\phi/2$ (base angle ϕ), measurements.

1). Compared to materials grown in the lower-temperature growth zone, the pyramidal tops of these structures typically have wider tip diameters of 13 ± 9 nm and shorter heights of 219 ± 52 nm (see the Supporting Information, Figure S3). However, the cone angles of these tips remain sharp (10.8 ± 2.2°). Although the length of these shorter tip obelisks is in general ~5 μm, their shaft is mostly of uniform width (85 ± 10 nm) with less than 20% variation over the entire length of the structure, which correlates to an angle of vertical declination at the base of 0.35 ± 0.15°. At the highest-temperature growth region (~960 °C) 5 cm away from the La precursor, LaB_6 nanowires were grown instead (images c and e in Figure 1). These wires were also capped by Pt particles and had diameter distribution of 30 ± 20 nm. Control experiments without the catalysts under the same conditions yielded only LaB_6 films instead.

The chemical identity and crystallinity of these LaB_6 nanoobelisks were examined by TEM and EDX elemental analysis. Figure 3 illustrates typical zoom-in TEM images of an obelisk tip. High-resolution TEM images along with the selected area electron diffraction patterns reveal the single-crystalline nature of the LaB_6 nanoobelisks with exhibited lattice spacing of ca. 4.15 Å (images a and b in Figure 3). The growth directions of these nanostructures are determined to be mostly along the [001] direction. Dark regions, indicative of a high z material, are found at the ends of most obelisks and wires. Elemental mapping of the obelisk by EDX confirms the presence of boron and lanthanum in the appropriate regions of these obelisk structures (Figure 3c and the Supporting Information, Figure S4). The silicon signal in the EDX spectrum is attributed to background contaminations from silicon substrates as suggested by findings in other metallic boride synthesis.[19] The copper signal is from the copper TEM grid. The EDX spectrum at the edge of the nanoobelisk also reveals the identity of the

(18) Henglein, A.; Ershov, B. G.; Malow, M. *J. Phys. Chem.* **1995**, *99*, 14129.

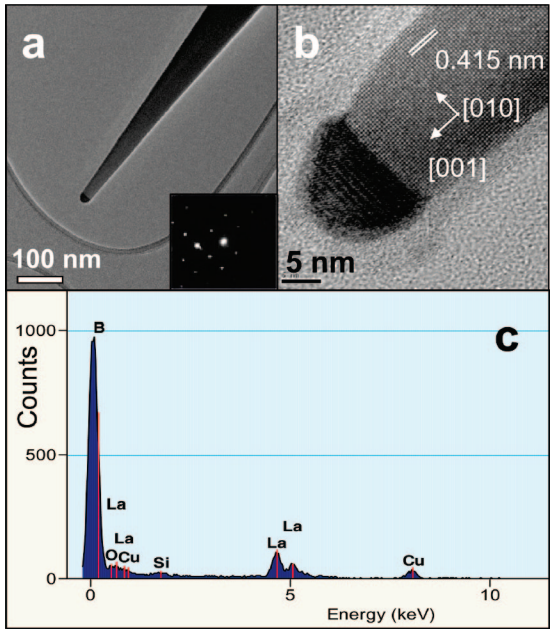

Figure 3. TEM images of a LaB_6 nanoobelisk at (a) low and (b) high resolution. (inset) Selected area electron diffraction pattern obtained at the LaB_6 area of an obelisk tip. (c) EDX spectrum measured at the bulk shaft of a typical obelisk.

thin amorphous coating, typically several nanometers thick, to be overcoated boron. The EDX spectrum at the obelisk tip indicates that the dark region is a Pt-rich material containing boron and lathanum, suggesting that a vapor–liquid–solid growth mechanism may be involved in the material's growth (see the Supporting Information, Figure S4).

A time trial growth study was conducted for further insight into the growth of the obelisk structures at 920 °C. Structures of samples with reaction duration periods of 3, 5, 9, and 13 min were analyzed using SEM (see the Supporting Information, Figure S5). Figure S5e depicts a schematic of a possible growth mechanism for the nanoobelisks. Initially, a thin layer of cubic-shaped polycrystalline film of LaB_6 was deposited on the silicon substrate coated with Pt particles. Some Pt particles migrated to the faceted surfaces of these cubic crystals and catalyzed the growth of LaB_6 nanowires. These vapor-saturated particles were elevated off the substrate as the wires were formed via the typical VLS process.[20] During the 5–9 min growth period, the observed increases in the heights and widths of the materials suggests the growth process followed a continuous VLS type vertical growth with lateral growth due to secondary deposition. The competition between this slow secondary deposition and vertical growth likely initiated the development of tapered wires (see the Supporting Information, panels b and c in Figure S5). The evolution of these wires into obelisk structures occurred between the 9 and 13 min reaction period (see the Supporting Information, Figure S5d). As this sample was in proximity to the $LaCl_3$ precursor, it received high precursor flux, which contributes to the large base widths of obelisks and faster lateral growths.[19] Once the $LaCl_3$ precursor was significantly depleted, the local concentration at the growth zone decreased until the remaining precursor flow was completely exhausted. This decrease in concentration was expected to cause a decrease in the ratio of lateral vs vertical growth, leading to the growth of pyramidal tops of the obelisks. Although this proposed multistage growth model is qualitative because of the finite time needed for the complete depletion of precursor materials at the end, it is consistent with observations in growth experiments such as the multistage growth of zinc oxide nanotips on flat top nanowires.[21]

Another indication of this pyramidal top growth due to the change in precursor flux could be inferred from the structures of materials grown in reaction zones with a faster halt in precursor concentration. Because the on-start decomposition temperature of decaborane is low (170 °C), most of the decaborane decomposes at the upstream of the furnace. Thus, the flux of decaborane reaching the sample is much smaller at positions located further downstream, and less secondary deposition is expected. This implication is verified by the uniform shaft dimension of obelisks with shorter pyramidal top obtained at 945 °C (images b and e in Figure 1). These results are in line with the expectation of shorter pyramidal growth time with a faster depletion of source materials after the precursor shutoff in the down stream regions. Growth of only flat-topped, uniform-diameter LaB_6 nanowires farther downstream further illustrates the importance of precursor flux change in the geometries of material tip growth. The present type of material growth mode, as compared to kinetically favored growth of specific facets that allows for only fixed cone angles,[9] lends us the possibility to modulate the cone angles of nanostructures by varying the local change in precursor flux. Nevertheless, we cannot eliminate crystal dislocations as possible explanations for this pyramidal top growth. Yet further HRTEM studies at the ~50 nm long pyramid-shaft interface were ineffective because of the large sample thickness.

In conclusion, metal-catalyzed CVD growth of single-crystalline LaB_6 nanoobelisks of different pyramidal top heights was achieved via a postulated multistage growth model. Our time trial study suggests that a large change in precursor flux and temperature variations is necessary to create these obelisk structures. Further study of these structures is being conducted to reveal the effect of geometry on their field-emission properties and Raman scattering. We expect that this work will spur further interest and investigations of morphological control of nanostructures and their properties.

Acknowledgment. C.L.C thanks the support of Nebraska Research Initiative. We also thank the Nebraska Center for Materials and Nanoscience and Center for Biotechnology for the use of their facilities.

Supporting Information Available: Microscopy images, EDX spectra, and statistics of nanoobelisks measurements (PDF). This material is available free of charge via the Internet at http://pubs.acs.org.

CM702315X

(19) Xu, T. T.; Zheng, J.-G.; Nicholls, A. W.; Stankovich, S.; Piner, R. D.; Ruoff, R. S. *Nano Lett.* **2004**, *4*, 2051.
(20) Wagner, R. S.; Ellis, W. C. *Appl. Phys. Lett.* **1964**, *4*, 89.
(21) Yea, Z. Z.; Huang, J. Y.; Xu, W. Z.; Zhou, J.; Wang, Z. L. *Solid State Commun.* **2007**, *141*, 464.